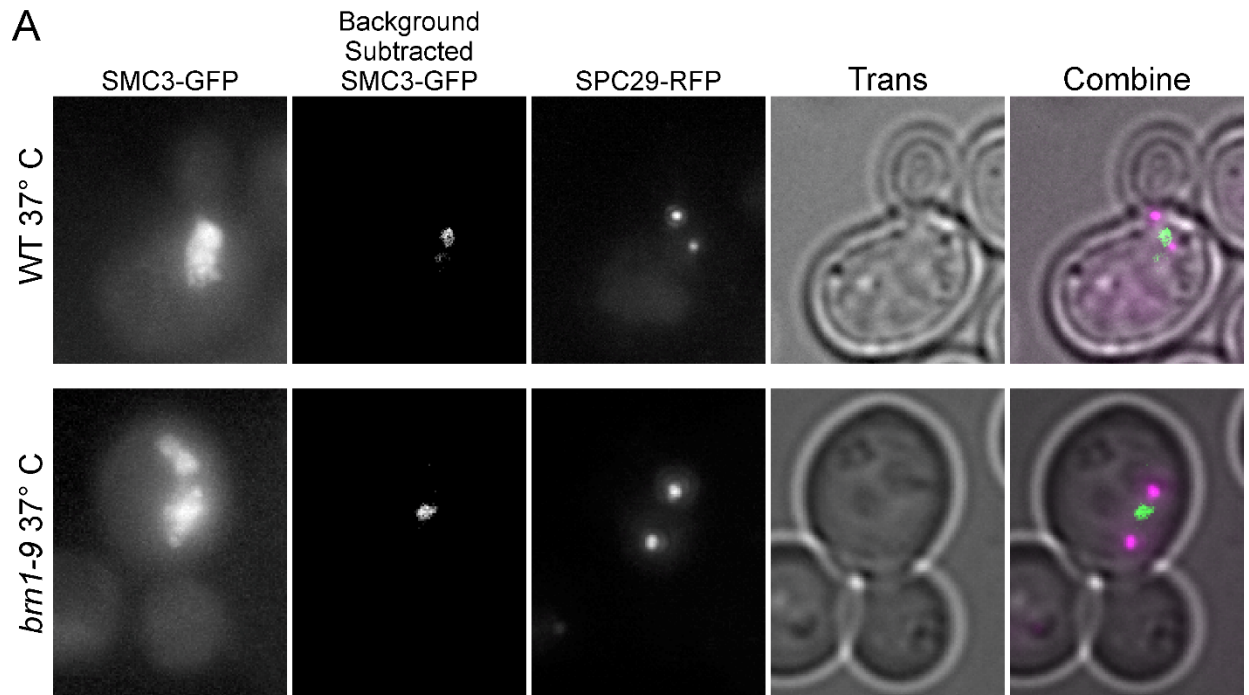


Supplemental Materials

Molecular Biology of the Cell

Lawrimore et al.



B

Strain	Enrichment Frequency Replicate 1 (enriched/total)	Enrichment Frequency Replicate 2 (enriched/total)	Enrichment Frequency Replicate 3 (enriched/total)	Mean Enrichment Frequency
WT	0.98 (39/40)	1 (32/32)	1 (33/33)	0.99
<i>brn1-9</i>	1 (31/31)	0.96 (26/27)	1 (29/29)	0.99

Figure S1. The temperature sensitive *brn1-9* condensin allele does not disrupt cohesin pericentric enrichment. (A) Representative images of SMC3-GFP and SPC29-RFP in WT and *brn1-9* cells grown at 37° C. SMC3-GFP images and SCP29-RFP images are maximum intensity projections. The Trans image is an in-focus plane. In the 'Combine' panels the SMC4-GFP is green, SPC29-RFP is magenta, and the Trans image is grey. (B) Table of pericentric cohesin enrichment across three technical replicates.

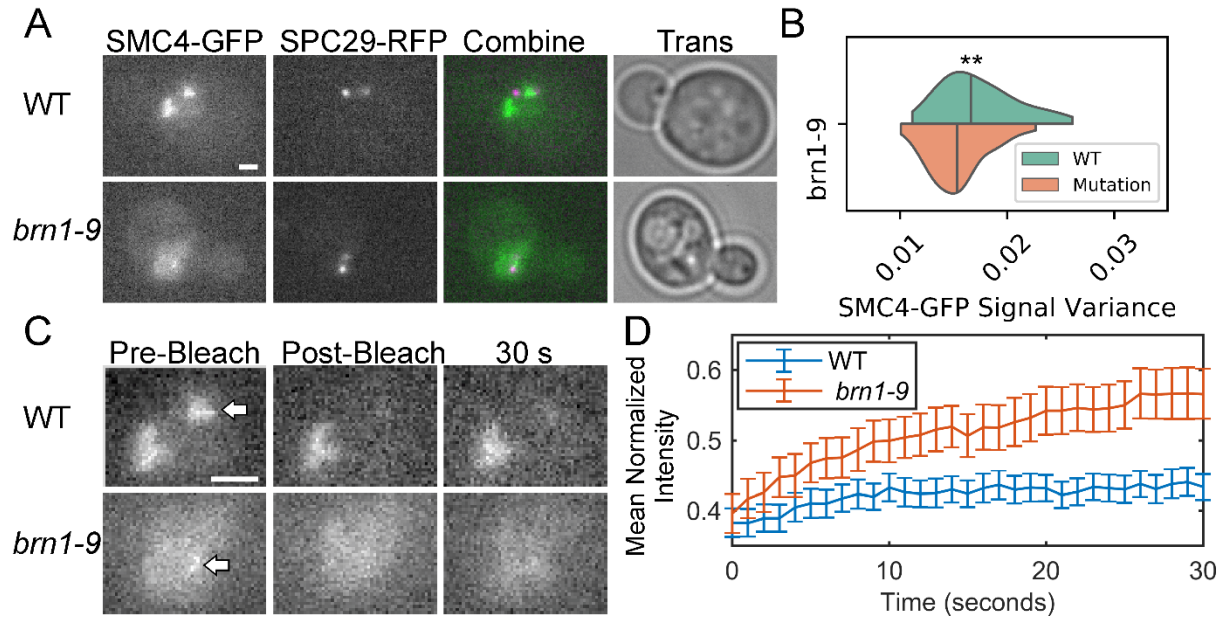


Figure S2. Temperature sensitive allele, *brn1-9*, reduces enrichment and increases turnover of pericentric SMC4-GFP. (A) Representative images (in-focus planes) of labeled condensin subunit, SMC4-GFP (green), and SPB protein, SPC29-RFP (magenta) in budding yeast during metaphase. Scale bar is 1 μm . (B) Violin plot of GFP signal variance in WT cells versus *brn1-9* cells. Wilcoxon rank-sum test (two-sided) p-values: WT vs *brn1-9* = 0.004. (C) Pre-bleach, post-bleach, and 30 s post bleach images of cells shown in A. Images are enlarged compared to A. White arrows indicate the bleached region centered on the pericentric region between the spindle pole bodies. Scale bar is 1 μm . (D) Mean normalized intensity recovery curve for pericentric SMC4-GFP. WT n = 51, *brn1-9* n = 38 timelapses. Error bars are SEM.

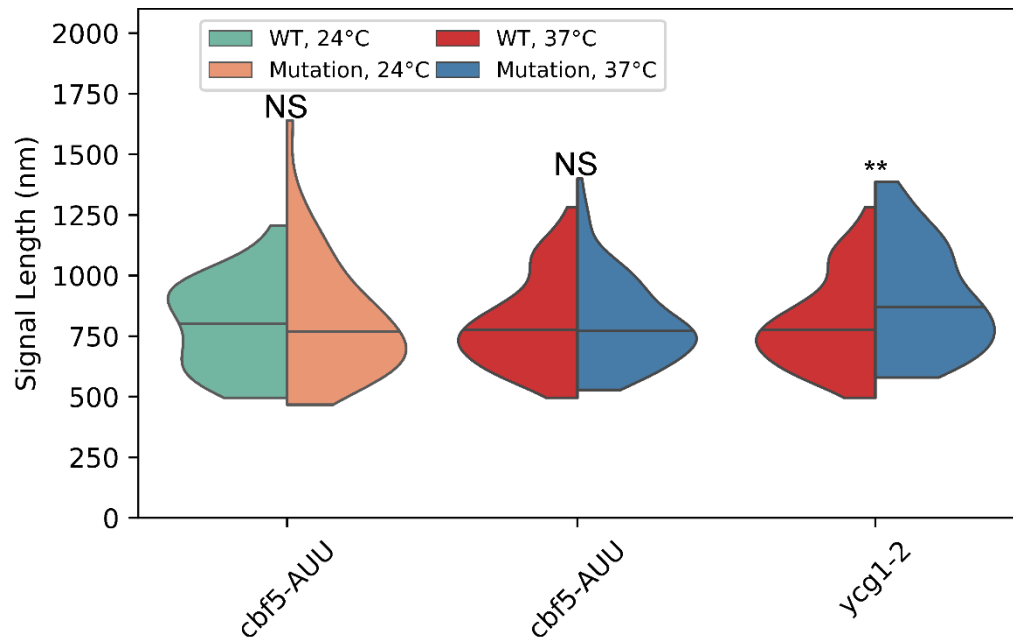


Figure S3. Disruption, not depletion, of pericentric condensin increases the tetO/TetR-GFP signal length of the dicentric plasmid pT431 in metaphase cells. Violin plot of the signal lengths of the tetO/TetR-GFP array in cells containing the dicentric plasmid pT431. Black line is the median of the distribution and the colored shapes are smoothed histograms of the distribution of signal length for each strain. Signals were measured from population images of metaphase cells. Metaphase cells were defined by a spindle length of less than 2 μm . WT 24° C n = 36, *cbf5-AUU* 24° C n = 45, WT 37° C n = 91, *cbf5-AUU* 37° C n = 86, and *ycg1-2* 37° C n = 67. Wilcoxon rank-sum test (two-sided) p-values compared to WT at corresponding temperature: *cbf5-AUU* 24° C = 0.9, *cbf5-AUU* 37° C = 0.9, and *ycg1-2* 37° C = 0.003. Multiple comparisons of WT 37° C to mutants was corrected using Bonferroni correction.

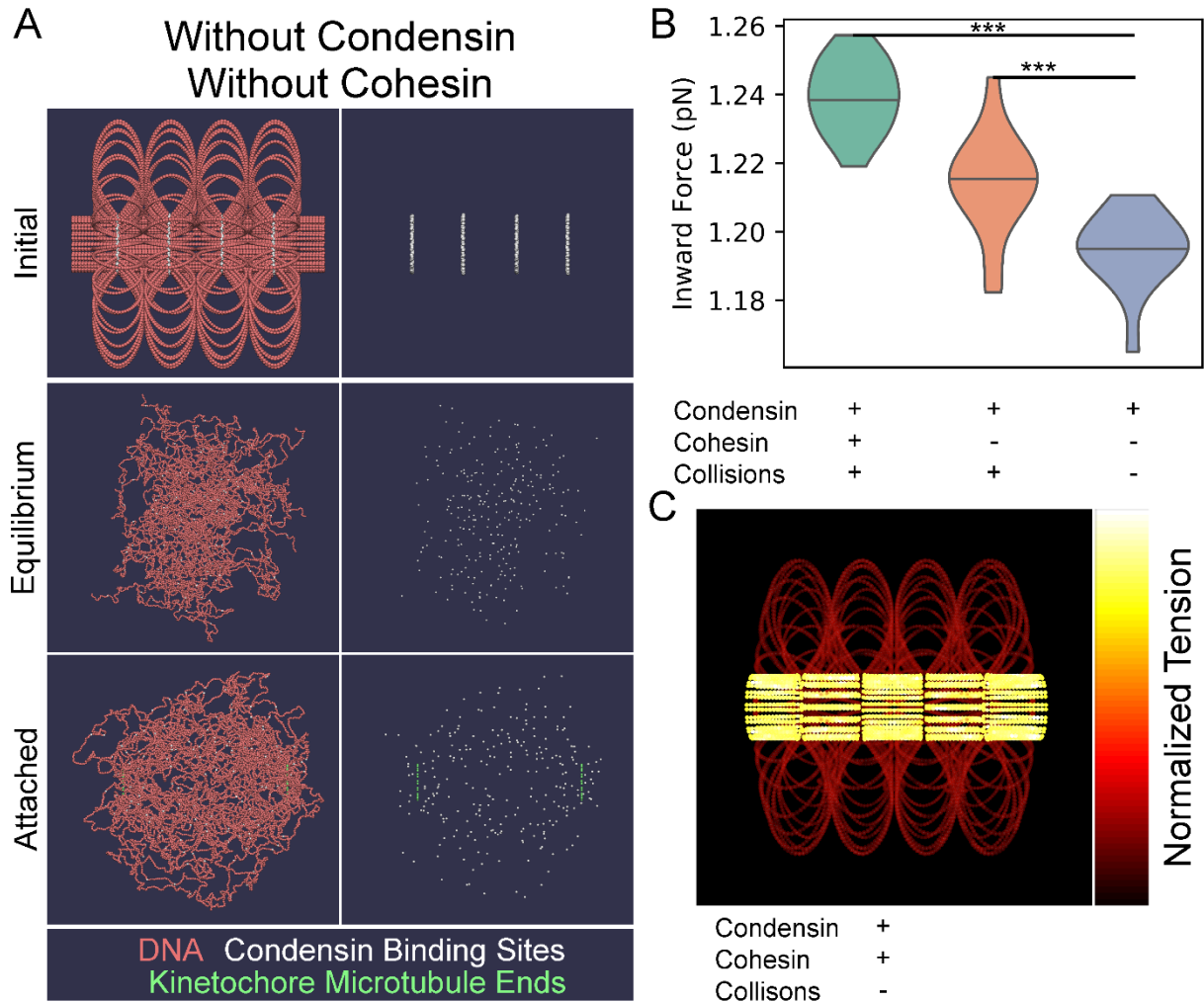


Figure S4. Visualization of simulations without condensin, cohesin, or collisions. (A) ChromoShake simulation of pericentromere with neither cohesin nor condensin. Initial configuration is in upper panels. Centromeres, the leftmost and rightmost beads, are separated by 800 nm. Middle panels correspond to timepoints indicated by black arrows in Fig. 7 B. Lower panels correspond to final timepoints in Fig. 7 B. Each panel is also shown without DNA for clarity. Condensin binding sites are in white and are in each panel. (B) Violin plot of inward force in pericentromere simulations with permanent attachment to kinetochore microtubules. Black line is the median of the distribution and the colored shapes are smoothed histograms of the distribution of the inward forces for each simulation type. Cohesin function is dependent on collisions in simulation. All simulations contained $n=16$ sister centromere pairs. Wilcoxon rank-sum test (two-sided) p-values: with cohesin and with collisions vs without cohesin and without collisions = 2×10^{-6} , without cohesin and with collisions vs without cohesin and without collisions = 4×10^{-4} . (C) Initial configuration of pericentromere simulation with permanent attachment to kinetochore microtubules where DNA beads are colored based on the mean tension on each bead after the simulation has run for 0.05 s of simulation time. The simulation contains cohesin and condensin, but lacks collisions, eliminating any effects from molecular crowding. The bead with the most tension in each simulation white, while the bead with the lowest tension is black. The leftmost and rightmost beads are not shown.

Strain Name	Relevant Genotype
KBY9035-2	(YEF 473A) Smc4-GFP:Kan, Spc29-RFP:Hyg
AYY1003-1	(YEF 473A) brn1-9:Nat, Spc29-RFP:Hyg, Smc4-GFP:Kan
KBY9471-1	(YEF 473A) Spc29-RFP:Hyg, SMC3-GFP:Ura
KBY9076-1	(YEF 473B) Smc3-GFP:Ura, Spc29-RFP:Hyg, brn1-9:Nat
KBY8065	MATa CEN15(1.8)-GFP[10kb] ade2-1, his3-11, trp1-1, ura3-1, leu2-3,112, can1-100, LacINLSGFP:HIS3, lacO::URA3, Spc29-RFP:Hyg
KBY9059-1	MATa CEN15(1.8)-GFP[10kb] ade2-1, his3-11, trp1-1, ura3-1, leu2-3,112, can1-100, LacINLSGFP:HIS3, lacO::URA3, Spc29-RFP:Hyg, mcm21Δ:Nat
KBY9040-1	MATa CEN15(1.8)-GFP[10kb] ade2-1, his3-11, trp1-1, ura3-1, leu2-3,112, can1-100, LacINLSGFP:HIS3, lacO::URA3, mcd1-1, Spc29-RFP:Hyg
KBY9039-2	MATa CEN15(1.8)-GFP[10kb] ade2-1, his3-11, trp1-1, ura3-1, leu2-3,112, can1-100, LacINLSGFP:HIS3, lacO::URA3, Spc29-RFP:Hyg, brn1-9:Nat
JLY1074-1	MATa CEN15(1.8)-GFP[10kb] ade2-1, his3-11, trp1-1, ura3-1, leu2-3,112, can1-100, LacINLSGFP:HIS3, lacO::URA3, Spc29-RFP:Hyg, cbf5-AUU:Nat
JLY1039-1	(W303) Mat A trp1::MET-Recombinase::TRP leu2::TetR-GFP::LEU2, Spc42-mCherry:Kan, pT431 #9
JLY1043-1	(W303) Mat A trp1::MET-Recombinase::TRP leu2::TetR-GFP::LEU2, Spc42-mCherry:Kan, mcm21Δ:Kan, pT431 #9
JLY1062-1	(W303) Mat A trp1::MET-Recombinase::TRP leu2::TetR-GFP::LEU2, Spc42-mCherry:Kan, brn1-9:Nat, pT431 #9
JLY1056	(W303) Mat A trp1::MET-Recombinase::TRP leu2::TetR-GFP::LEU2, Spc42-mCherry:Kan, ycg1-2:Kan, pT431 #9
JLY1041-1	(W303) Mat A trp1::MET-Recombinase::TRP leu2::TetR-GFP::LEU2, Spc42-mCherry:Kan, cbf5-AUU:Nat, pT431 #9
KBY8159-1	MATa ade1, met14, ura3-52, leu2-3,112 his3-11,15 lys2Δ::lacI-GFP-NLS-NAT, 1.1 kb CEN 3::LacOKAN (1.2-kb array), natΔ:His3
JLY1071-1	MATa ade1, met14, ura3-52, leu2-3,112 his3-11,15 lys2Δ::lacI-GFP-NLS-NAT, 1.1 kb CEN 3::LacOKAN (1.2-kb array), natΔ:His3, mcm21Δ:Nat
JLY1072-1	MATa ade1, met14, ura3-52, leu2-3,112 his3-11,15 lys2Δ::lacI-GFP-NLS-NAT, 1.1 kb CEN 3::LacOKAN (1.2-kb array), natΔ:His3, brn1-9:Nat

Table S1. Strain Genotypes.